

ISSN 0389-4010
UDC 531.788
533.59
533.6.011.8

TECHNICAL REPORT OF NATIONAL AEROSPACE LABORATORY

TR-1287T

High-Altitude Pressure Measurement in the Orbital Re-Entry Experiment (OREX)

Takashi Matsuzaki, and Yasutoshi Inoue

April 1996

NATIONAL AEROSPACE LABORATORY

CHÔFU, TOKYO, JAPAN

High-Altitude Pressure Measurement in the Orbital Re-Entry Experiment (OREX)*

Takashi Matsuzaki*¹ and Yasutoshi Inoue*¹

ABSTRACT

The first Japanese Orbital Re-entry Experiment (OREX) that successfully flew was launched by the first flight of an H-II rocket on February 4, 1994, and was inserted into a circular orbit at about 450km. The OREX acquired experimental data during its orbital flight and re-entry. The OREX project was conducted as a joint effort between the National Aerospace Laboratory (NAL) and the National Space Development Agency of Japan (NASDA).

Pressure data along the flight trajectory is among the most important and fundamental of the aerodynamic data. NAL took charge of the pressure measurement, as one of various measurement missions, from vacuum at high altitude down to an altitude of about 75km with a four-decade precision capacitive-type pressure transducer. These data can be used to predict the surface pressure and the ambient pressure in similar flights in the future. The data verified the real gas Computational Fluid Dynamics (CFD) codes through comparison with aerodynamic calculation results.

This paper outlines the design, fabrication, performance tests, environmental tests, flight operation, flight data and their evaluation of high altitude pressure measurement systems.

Key Words : Re-entry, Aerothermodynamics, Rarefied-gas, Pressure measurement, HOPE

概 要

日本最初の軌道再突入実験 (OREX) は、平成6年2月4日にH-IIロケット試験機1号機によりOREX機体が高度450kmの円軌道に投入されて始まり、予定通りに一周回飛行した後に軌道離脱を行い、大気圏再突入時の飛行データが取得された。OREXは、航空宇宙技術研究所 (NAL) と宇宙開発事業団 (NASDA) が共同研究で進めてきたHOPE研究開発の一環である飛行実験プロジェクトの一つである。

NALは、OREXの目的の一つである熱空気力学計測ミッションを分担して、センサやプローブ等を搭載した。これにより大気圏再突入時の空力環境データの取得、再突入時に発生する高温電離・解離気体の特性データを取得し、CFD (計算流体力学、スーパーコンピュータなどによる大規模数値シミュレーション) の計算コードなどの飛行実証を行うことが目的である。

大気圏再突入時の高々度圧力計測は、希薄気体領域から近連続流領域までの merged layer 機体壁面圧力をOREX機の表面部材に設置された隔膜静電容量型圧力計により4桁の範囲で計測する。高々度圧力計測は、再突入初期の高々度領域での微小加速度及び壁面圧力の計測から希薄気体熱空力環境予測法を評価することと一様流状態量を推定するために行った。また希薄気体CFDコードの検証に供される。

* 平成8年2月22日 受付 (received 22 February 1996)

*¹ 空気力学部 (Aerodynamics Division)

1. Introduction

Japan's first orbital re-entry experiment (OREX) was started when an OREX vehicle was projected onto a circular orbit at an altitude of 450km by a prototype No.1 of H-II rocket in February 4, 1994. Break-off from the orbit was made after an orbital flight was finalized as scheduled, and flight data during re-entry into the atmosphere were obtained. The OREX plan is one of series of the flight experiments forming the HOPE research and development program promoted jointly by National Aerospace Laboratory (NAL) and National Space Development Agency of Japan (NASDA).

NAL is in charge of an aerothermodynamic measurement mission which is one of the purposes of OREX, and is engaged in equipping devices such as sensors, probes, etc. upon the body. With the aid of these devices, aerothermodynamic environmental data at the re-entry into the atmosphere are to be obtained. Furthermore characteristic data of the high temperature ionized/dissociated gases generated at the re-entry are obtained. Thus it is intended that flight validation including codes of CFD (large-scale numerical simulation of fluid dynamics by super computer) will be made.

High-altitude pressure measurement at the re-entry of OREX into the atmosphere is made with the body wall surface pressure in the merged layer region by means of a diaphragm electrostatic capacitance pressure gauge equipped upon the sur-

face structure of the OREX vehicle ranging to 4 decades. The high-altitude pressure measurement was made in order to evaluate the rarefied-gas aerothermodynamic environment prediction method and to estimate an amount of gas properties of uniform flow. On the other hand, the measurement is also offered for verification of rarefied-gas CFD codes.

2. Experimental project

A schematic diagram of the flight plan of OREX is shown in Fig. 1. OREX is to be launched from Tanegashima Space Center by means of the prototype No. 1 of H-II rocket, and is to be thrown into a circle orbit at an altitude of approximately 450km. OREX having finished an orbital flight of its own is to break off from its orbit by making retro-jetting, and is to re-enter the atmosphere by gradually lowering its altitude. During and after the re-entry, measurement is made with the factors affecting the state of the gas by means of the sensors attached to the individual portions on the vehicle. The data covering the duration of time of approximately 210sec corresponding to the flight path ranging from the altitude approximately 120km to the altitude 38km are to be recorded, as well as telemetered, in the data memory equipped onto the vehicle. With the data taken out from these sensors via a signal conditioner, not only sampling is to be made at 1.25Hz in the telemeter package but also digital conversion is to be made

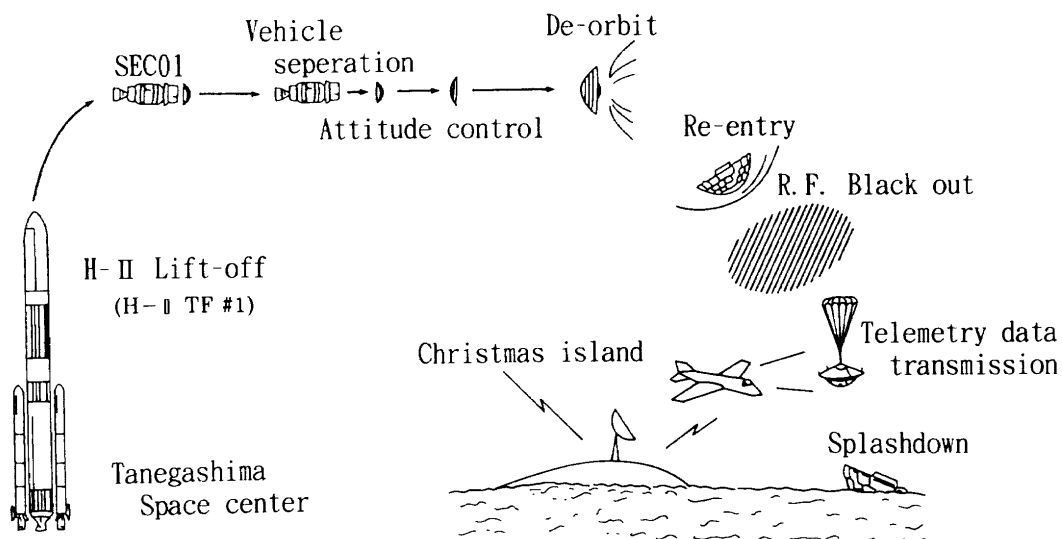


Fig. 1 Sketch of OREX flight profile

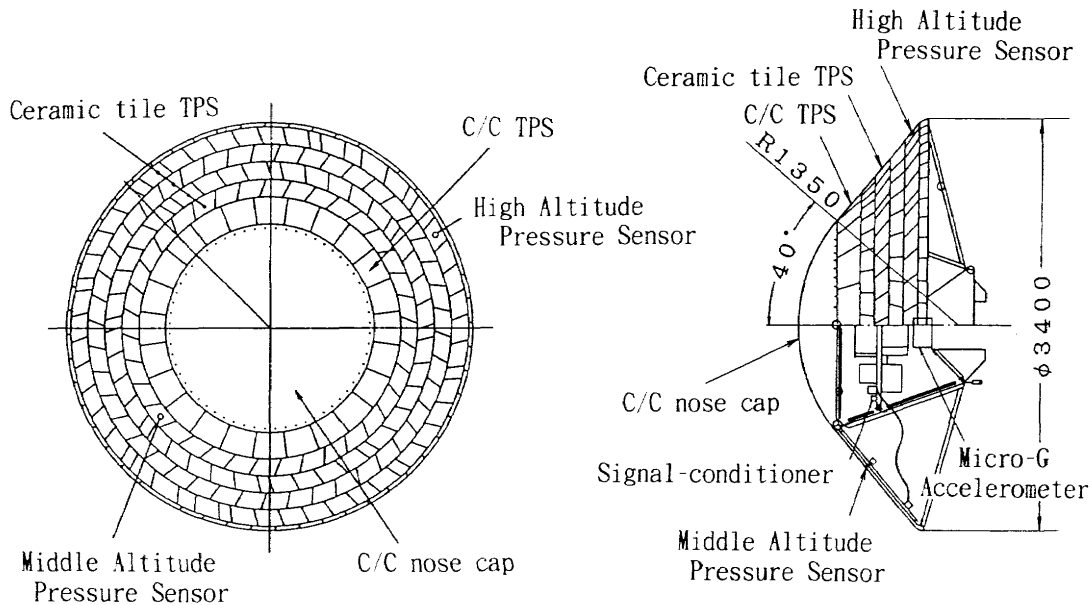


Fig. 2 Schematic diagram of OREX vehicle

with an 8-bit analog/digital convertor, and transmission is made at real time by a VHF transmitter. In addition to the above, the data obtained during the term of the blackout (a phenomenon of communication being disrupted) and those recorded during an invisible region from the ground-based stations are to be reproduced and retransmitted at three times faster than when recorded at an appropriated period after the blackout is over. A schematic diagram of OREX is shown in Fig. 2. The vehicle in question is of the blunted-cone shape with a spherical head, and a carbon-carbon material, ceramic tiles, etc. as heat-resistant and heat protective materials which are to be used also for HOPE are used for the front part of the vehicle to be exposed to aerodynamic heating at the re-entry. Ensuring performance of such materials is included in OREX's purpose. Each of electronic equipment is protected from heat or temperature by being placed in an exclusive part in the inside of the vehicle.

The re-entry into the atmosphere driven by such orbital speed is the first attempt in Japanese space development program. Space Shuttle and Brun have already been operated by the United States and Russia, but information concerning these designs including detailed data is seldom publicized. However pressure measurement along the re-entry orbit with shuttles is already in publicized^{1) 2)}, and results of the measurement are re-

ferred for our experiment. Results of similar experiments for pressure measurement in rarefied-gas regions have been offered for reference³⁾. High-altitude surface pressure measurement is the consecutive measurement of the body wall pressure in the aerodynamic environment ranging from a rarefied-gas region to an almost continuum flow region to the extent between the altitude of more than 120km and the altitude of 75km by means of a high-altitude pressure sensor. A pressure inlet of the high-altitude pressure sensor is placed on a surface position of the 4th row of the ceramic tiles at the conical portion of the vehicle, and is introduced to the pressure gauge attached to the surface of the inside aluminum main structure. The high-altitude pressure sensor is located on a position shown in Fig. 2.

In this configuration, any disturbances to measured pressures due to gaps and steps between tiles (typically 0.5~1mm) can be neglected because the boundary layer is sufficiently thick (10~30cm) along the surface as shown by many experiments in the supersonic flow around $M=2$.

Details of the design and making of the whole of OREX are summarized in a report of "Completion of Experimental Development of Orbital Re-entry⁴⁾," or in "Study of HOPE (No. 15), the Orbital Re-entry Experiment (OREX)" edited by NAL/NASDA.

3. Development of measurement system

With equipment and apparatus such as sensors and signal conditioners aboard OREX, design for which reliability is secured as far as possible has been intended. Also with circuit systems of electric design and parts and components to be used, location of parts and components of which environment resistivity is taken account as far as possible is established with such ones enjoying reputation for use in space as kernel materials. With mechanical design, the sensor and components are provided with sufficient margin for given vibration and shock environment, and the structure with which weight and thermal/electromagnetic compatibility are in consideration is adopted. With thermal design, structure allowing the internal heat to be as homogeneously as possible dispersed and permitting heat to effectively transfer through the case surface is adopted.

3.1 Pressure gauges

With a flight path ranging from the altitude of approximately 120km to the altitude 75km after re-entry into the atmosphere, vehicle wall surface pressure prediction was made in accordance with CFD based on the standard atmospheric model before flight. Analysis was made at the altitude of higher than 95km in accordance with DSMC (direct simulation Monte Carlo method) and at the altitude of lower than 95km in accordance with Navier Stokes Code. A relation between the high-altitude wall surface pressure and the altitude is shown in Fig. 3. The \circ marks indicate the analytical values, whereas \square marks denote the extrapolation values. From the result of CFD, it is predicted that the measurable range is extended from approximately 0.533Pa (0.004 Torr) to 1.333kPa (10 Torr). Although pressure gauges were intended to be developed anew for OREX, shortage of the term was expected to prevent the development from being accomplished and compelled the conventional gauges to be employed with some remodeling.

To choose the pressure gauges equipped upon OREX, performance survey is made with Pirani gauges, ionization vacuum gauges, and

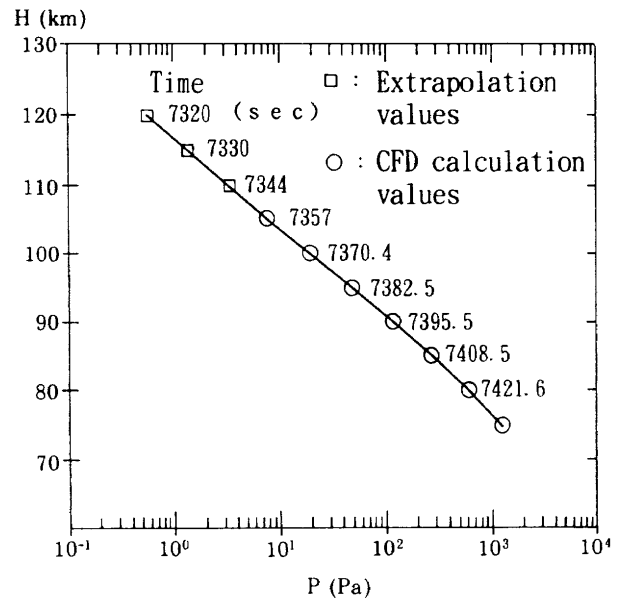


Fig. 3 High-altitude wall surface pressure versus altitude

mass spectrometers that have been used for measuring the pressure during the flight of rockets and artificial satellites together with spinning rotor vacuum gauges, diaphragm pressure gauges, etc. In consideration of the fact that the test is a flight experiment, especially of the fact of it being to be conducted under severe environment accompanied with the flight within the atmosphere at the speed of more than 7km/sec, diaphragm pressure gauges are chosen. Diaphragm pressure gauges are of the high-speed responsive type, and have, at the same time, excellent performance especially of high resolution, high accuracy, endurance, etc. After the investigation, it is determined that Edwards Co.'s Barocell-590 type that can be used for a standard gauge for rectification is to be used as the gauges to be equipped upon the prototype. Major performance of the gauge is listed in Table 1.

Remodeling was made with the gauge in question for the purpose of equipping it on OREX. However the electric circuits were excluded from the process of remodeling, because the circuits are concerned with guarantee of the performance of the pressure gauge. Major points of the remodeling are as described below.

- 1) Electric remodeling
 - a) IC, whose socket is removed, is directly sol-

Table 1 Performance of pressure gauge

Type	diaphragm capacitance type, absolute pres. type
Pres. range	0~1.333kPa (10Torr)
Accuracy	±0.15% of reading value, +0.001% of full scale
Diaphragm	material: Inconel, O.D.: 40φ, thickness: 10μ
Pres.-responsive time	8msec
Resolution	0.0133Pa (0.0001Torr)
Used temperature range	5°C~70°C
Weight	1kg

dered onto a printed circuit board.

- b) The electrolytic capacitors of the power source are exchanged for the ones to be used in space, i.e. for a tantalum-foil dry electrolytic capacitors.
- c) To secure isolation of the ground on the primary side of the power source, the box grounding circuit is removed.
- d) On the pressure gauge cover and on its back side, bonding treatment is made.
- e) The input/out connectors, which are designed for the use on the earth, is changed for being usable in the space.
- f) Variable resistors are fixed with a bonding agent in an adjusted configuration at the final stage of equipment.

Performance tests after remodeling will be referred to later.

2) Mechanical remodeling

- a) Parts surrounding sensitive portions and parts surrounding electric elements are potted (fixed with epoxy bond).
- b) The external panels are anew made.
- c) Reinforcement of the connecting part between the pressure inlet and the vehicle is made. Also a rigidity strengthening countermeasure is taken.

3. 2 Pressure measurement system

3. 2. 1 Orifice and inlet tube

In the vicinity of the altitude 120km, a rarefied-gas region with Knudsen Number $Kn \approx 1$ based on the wall surface pressure values predicted by CFD and the representative length of OREX should be found. A transition flow region

continues as far as the vehicle descends to the position around the altitude 95km, and either of the regions shows behaviors never appearing as if it were a continuous fluid. For pressure measurement of the rarefied-gas, a shape consisting of an orifice and cavity is used especially for free molecule flows^{5) 6)}. The wall surface pressure never becomes equal to the cavity pressure in the orifice until the ratio of the orifice thickness to the caliber is made small enough (in case of a free molecule flow and at an isothermal temperature). The orifice to be equipped onto OREX is of the type of the lid (0.1mm thick) whose peripheral edge is extremely sharpened around drilled $\phi 3$ mm hole. When an inlet pipe is used for measuring rarefied-gas pressure, the shape of the inletting portion or pipe and furthermore even internal wall temperature exerts influence on the pressure. Therefore there is a possibility that the pressure values exhibited are different from each other. To avoid such trouble, consideration was given to a method to attach a diaphragm of the pressure gauge directly onto the cavity by remodeling the conventionally-procurable pressure gauge. However such remodeling was after all found to be out of practicality because of the apprehension that performance of the pressure gauge is influenced. Circumstances compelled the inlet tube to be shortened as far as possible, and use of the cavity was out of consideration. However it is expected that an $\phi 8$ mm inlet pipe will concurrently play a role of the cavity complying with the orifice having a sharp $\phi 3$ mm lid. From this it can be said that the rarefied-gas molecules, which once rush into the inside, never rush out until they are adapted by colliding with the wall surface of the

inside time after time.

On the other hand in a region where the flow can be believed to be almost continuous at the altitude of less than 90km, the measured pressure values can be regarded as the ones of the pressure inlet regardless of whether an orifice is available or not.

Since the temperature of the pressure inlet tube becomes concerned directly with the pressure in a rarefied-gas region, measurement of the inside wall surface temperature is conducted by attaching a thermocouple onto the vicinity of the tube surface on a position at the depth of 40mm in the pressure inlet. The pressure inlet is made of stainless steel, and its external surface is covered with 0.15mm-thick zirconia by means of plasma spraying. Thanks to this treatment, the recombination

reaction of the dissociated atoms is also inhibited. Photographs of the front of the pressure inlet together with the pressure sensor and a schematic diagram of the pressure sensor are shown in Figs. 4, 5, and 6, respectively.

3. 2. 2 Pressure-responsive characteristics

1) Test unit

When pressure measurement is conducted on the OREX vehicle flying at high speed, the wall surface pressure is so rapidly and very widely varied as time lapses. In case of such a kind of pressure metrology, responsive time of the measuring system becomes to be an important factor. Especially in a rarefied-gas region, there might be a possibility that response is delayed. From this reason, it is intended that experimental assurance is

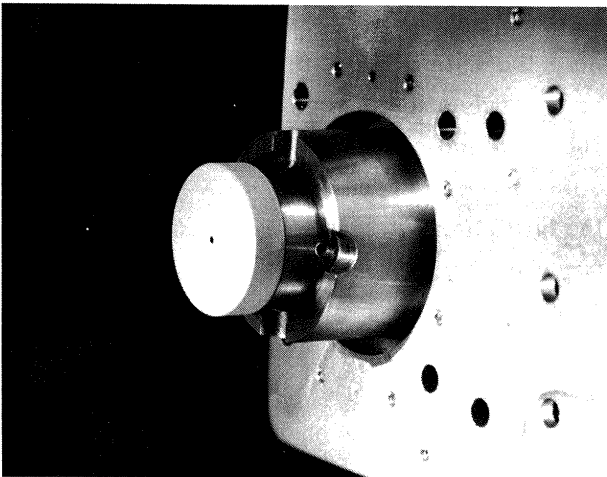


Fig. 4 Pressure inlet

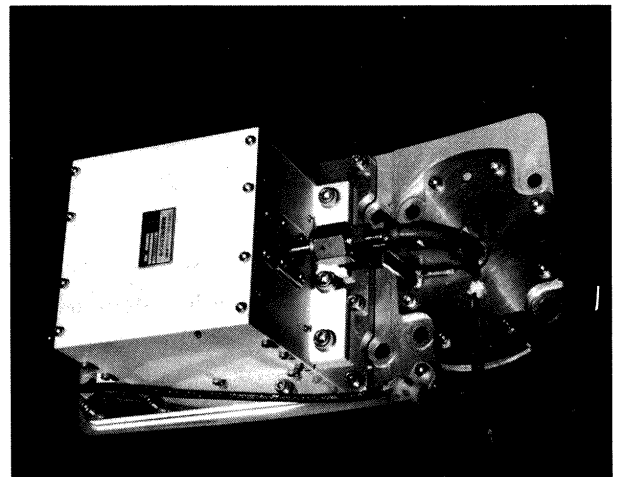


Fig. 5 Pressure sensor

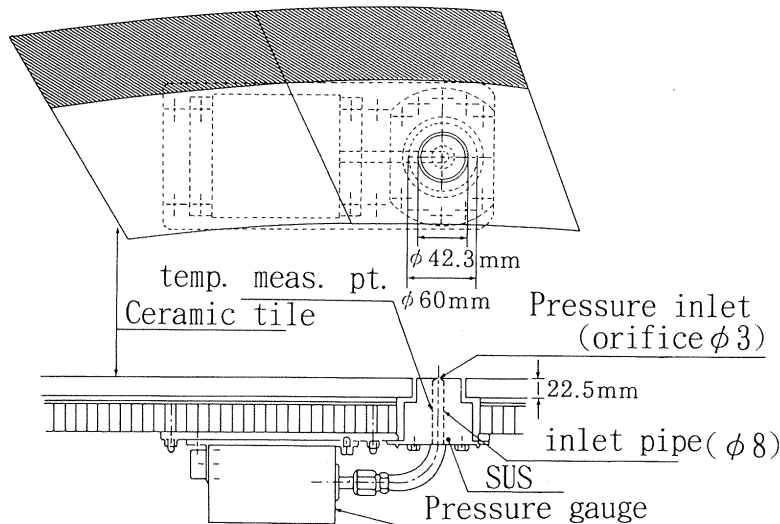


Fig. 6 Outline of pressure sensor system

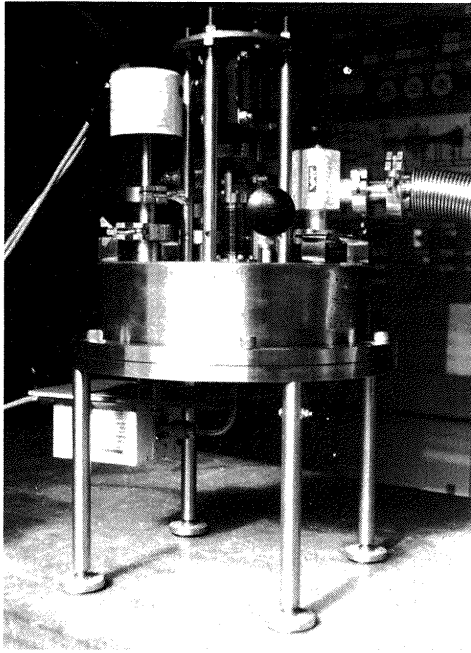


Fig. 7 Pressure-response test unit

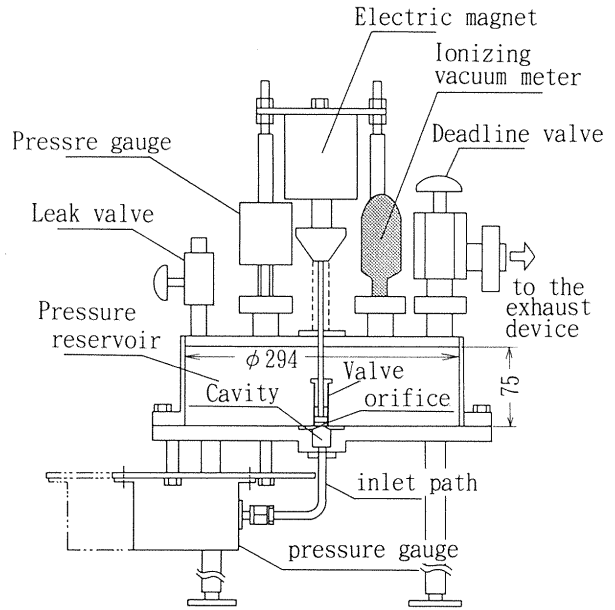


Fig. 8 Details of pressure-response test unit

made by building up a test unit like the experimental apparatus used in Literature 7. A photograph of the test unit is shown in Fig. 7, and a schematic diagram is illustrated in Fig. 8. The unit is comprised of a pressure reservoir, pressure inlet system (orifice, cavity, and inlet path), pressure gauge, exhaust device, leak valve, electric magnet, and valve. Stainless steel is the material for the unit. The pressure in the pressure reservoir and pressure inlet (=pressure measurement system) is reduced to the extent of the inlet-set pressure with the valves opened by simultaneously exhausting the gas by means of an exhaust device. At the next stage, the pressure in the inside of the reservoir is set to an arbitrary higher value with a valve and conduit orifice closed and with a leak valve gradually opened. After that, the valve is quickly opened and the pressure thus produced is instantaneously applied onto the pressure measurement system. The valve is opened and closed with an electric magnet. Metrology of the elevating speed of the valve with the electric magnet is made using a photo-transistor sensor. As a result, the speed is shown to be 1.5mm/msec. The pressure gauge the same type as the one equipped onto OREX is applied to the test. The set pressure range is approximately 0.0266Pa~60Pa, and air is used as the gas at room temperature.

2) Response time

The pressure gauge system responsive test was conducted with combination of the orifice caliber on the pressure inlet as 3mm, 5mm, cavity diameter as 20mm, 10mm, and depth 10mm as 20mm, and pressure inlet tube inner diameter as 6mm, 8mm. The length between the orifice and the pressure gauge is 214mm. To get the pressure response time, metrology is made with the process

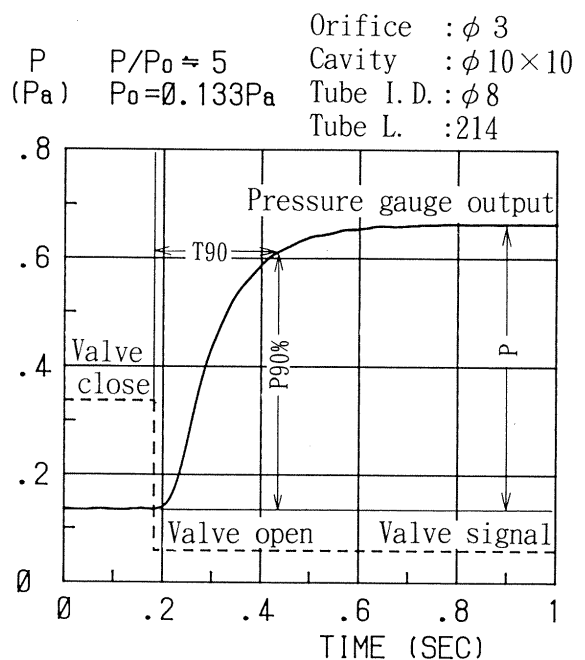


Fig. 9 Time-dependent change of pressure gauge output

of the measurement system pressure reaching the pressure arbitrarily set in the pressure reservoir. The measurement of the data is made using a data logger measurement device having the performance of A/D convertor with 12 bits, resolution $1 \mu V$, and sampling 5,000 times/sec. Time-

dependent change of the pressure gauge output in the rarefied-gas region is shown in Fig. 9. It is necessary for the response time required of the pressure measurement system to be given by duration of the period from opening of the valve in the pressure reservoir to the measurement chamber pressure reaching more than 99% of the difference of the pressures. However it is impossible to show the value with accuracy in an experimental manner, and therefore the value of 90% is given here. The required time for the measurement system pressure P_0 to reach 90% of the settled pressure P is shown in Fig. 10 (a, b, c).

From the correspondence between the high-altitude wall surface pressure by analysis shown in Fig. 3 and the time of seconds after launching, the pressure change ratio at the re-entry into the atmosphere is expected to be approximately 1.1 times per second. Such being the case, a pressure-responsive test was conducted by setting the pressure 1.1 times higher than the high-altitude wall surface pressure. The pressure piping system is of the same condition for equipping onto OREX of the orifice $\phi 3\text{mm}$ and inlet tube inner diameter $\phi 8\text{mm}$. The time-dependent change obtained from the above is depicted in Fig. 11. Here, the required time for the measurement system pressure P_0 to reach 95% of the set pressure P is obtained as the

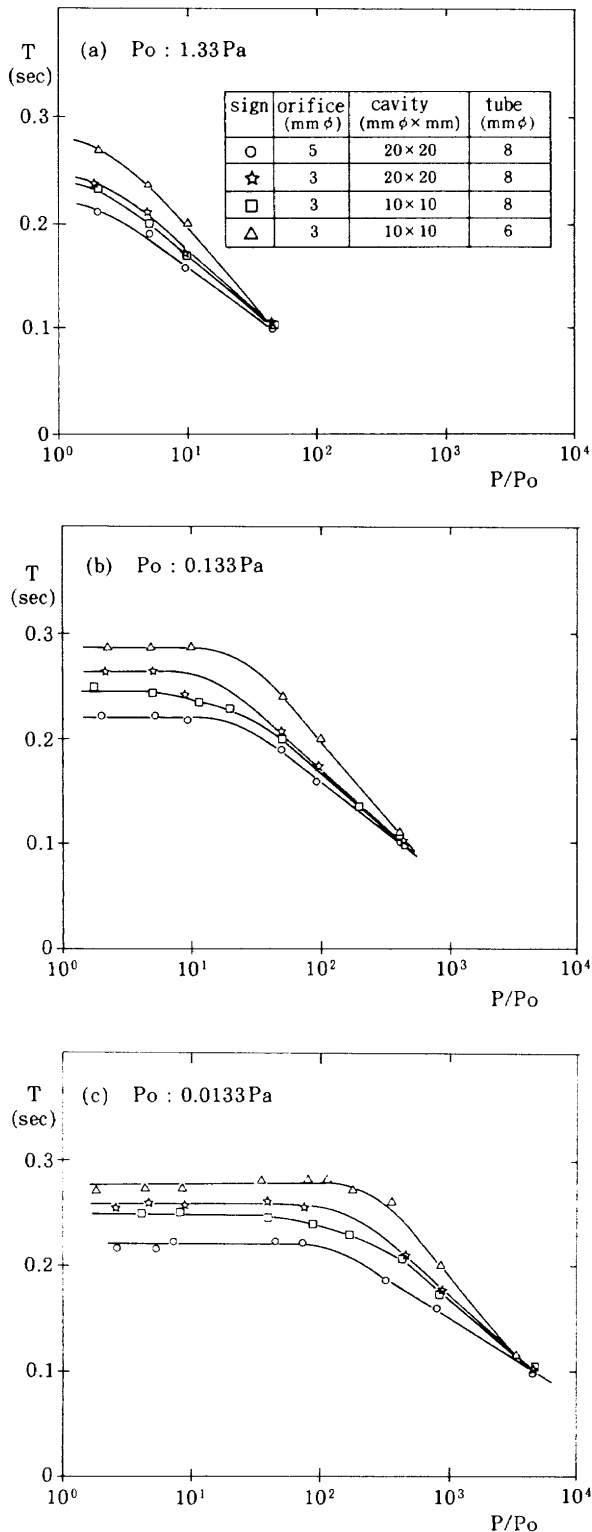


Fig. 10 Set pressure (90%) and response time

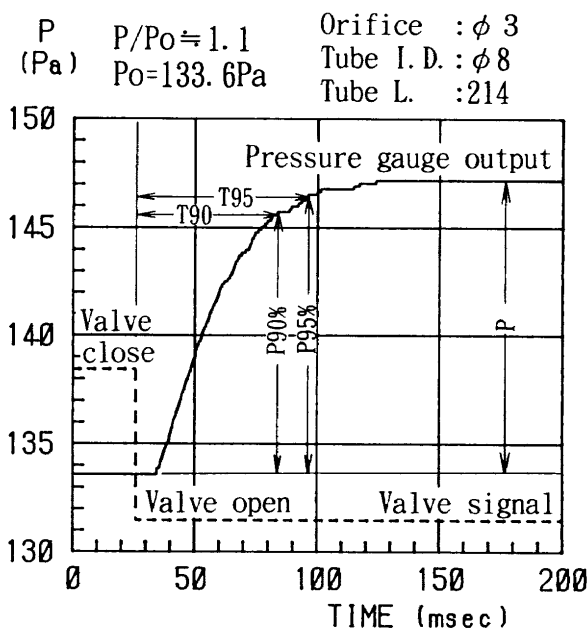


Fig. 11 Time-dependent change of pressure gauge output for step input

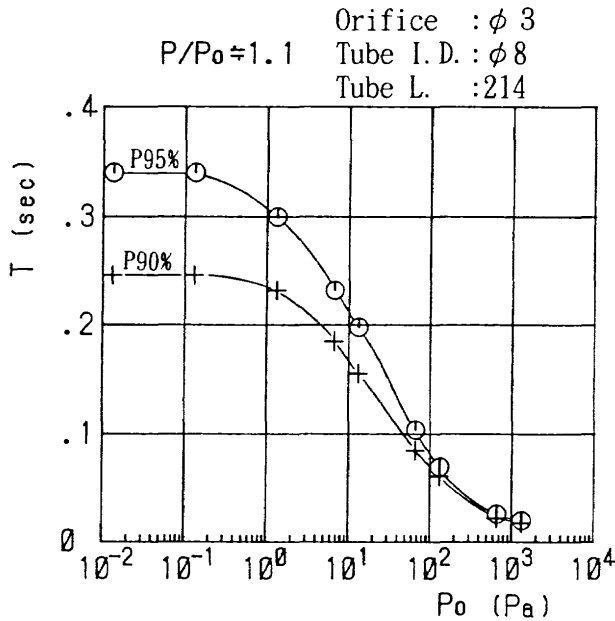


Fig. 12 High-altitude wall surface pressure and response time

pressure-response time in order to infer the instantaneous pressure values from flight data as accurately as possible. A relation between the result of the said required time and the high-altitude wall surface pressure complying with the altitude 120km~75km is shown in Fig. 12. The \circ marks indicate the required time for 95% of the set pressure. From this, 0.34~0.014sec is obtained as the pressure-response time (P95%) equivalent to 1.1 times of the high-altitude wall surface pressure 0.01~13.3Pa.

In the high-altitude region on the expected re-entry orbit, the altitude changes linearly with time. It is widely known that atmospheric pressure changes almost exponentially with the altitude. From this it is comprehended that the pressure-response time of the cavity takes not longer than 0.34sec. Thus it is permissible to state that the pressure measured at the time retrospectively prior to 0.34sec is to be the instantaneous value of the applied pressure being time-dependently constant. However during the flight of OREX, the applied pressure is estimated to be increased by 2% after 0.34sec. This means that intermediate pressure between the pressure (estimated to be reduced 2%) at the time retrospectively prior to 0.34sec and the pressure at present is measured. The slippage (deviation) between 2%~0% can

be regarded as measurement error.

3.3 Signal conditioner

The signal conditioner (hereafter abbreviated as S/C) was anew designed and constructed for equipping it onto OREX.

The S/C for pressure sensing has a function to allow measurement signals of the pressure sensor to be signal-rectified and to be low-pass filtered. Thus the signals are outputted onto telemeter package of an OREX measurement mission system. With the pressure measurement system, the sensor output is the voltage and is provided onto a normal voltage amplifying circuit. However since the signals of the pressure sensor is grounded to a casing in the inside, it is necessary for the grounding to be separated from the OREX system ground. Therefore as the primary step of the S/C device, an insulated amplifier was adopted.

With the telemeter package, the voltage with inputted voltage 0~5.1V is digitally converted by an analog/digital/convertor (A/D/C) to 8 bits. With the output of the high-altitude pressure sensor, the minimum resolution becomes 5.23Pa/count from the conversion factor 0.02V/count when output is made onto the telemeter package using a linear amplifier. With the high-altitude pressure measurement, measurement of 0.53Pa is predicted at the altitude of 120km. To extract significant pressure values from digital information of the telemeter package, improvement of the resolution was intended using a 3-decade logarithmic amplifier.

An ideal relation of the voltage output V_{out} to the voltage input V_{in} of S/C using a 3-decade logarithmic amplifier is given as shown below.

$$V_{out} = \frac{5.1}{3} \{ \log(V_{in}) + 2 \} \quad (1)$$

If the input voltage range of S/C using a 3-decade logarithmic amplifier is adjusted to 0.01~10V and the output value is adjusted to the input voltage of the telemeter package, then the minimum resolution of the high-altitude pressure measurement is 0.0366Pa. Thus it is noticed that the said resolution is heightened 142 times compared with the case of a linear amplifier. The S/C

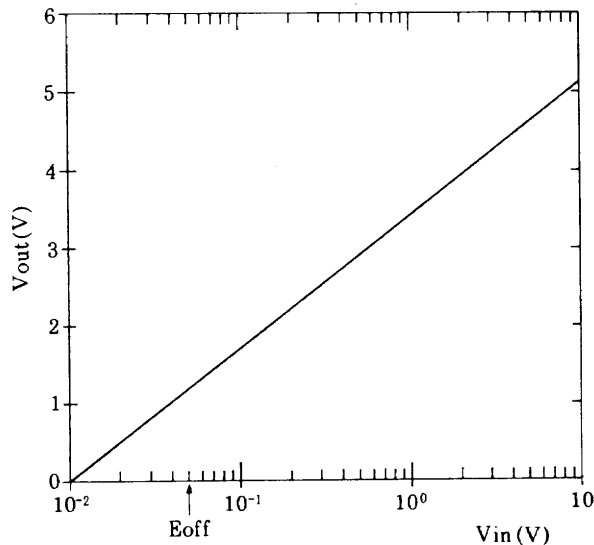


Fig. 13 Characteristics of signal conditioner

used for resolution improvement of the high-altitude pressure measurement changes its resolution by an off-set value E_{off} of the pressure sensor at the pressure $P \approx 0$. With the characteristics of the S/C shown in Fig. 13, the resolution is enhanced as E_{off} becomes smaller or the value approaches the input voltage of S/C. In the meantime, the resolution is deteriorated as E_{off} is made greater. Regarding the off-set value of the pressure sensor, it is necessary to determine the optimum value by ensuring the possible variation width in an environment test.

With a low-pass filter as a countermeasure of the electric noise, its cut-off frequency was determined to be 0.32Hz also out of necessity by an in-

formation theory corresponding to the fact that a sample rate on the telemeter package of OREX is 1.25Hz.

With the power source of the pressure sensor, care has been taken not to allow any trouble of the pressure sensor to be propagated to the OREX system by installing a DC/DC convertor and an overcurrent limitation circuit in the side of this unit, taking account of the fact that no safety design for the installed equipment has been evaluated.

With the S/C for the temperature sensor, the pressure inlet temperature sensor and the other temperature sensors are alternately switched with a multiplexer. Output obtained from the above is fed via an amplifier by performing temperature rectification with a cold-junction temperature to the telemeter package. As a temperature sensor to measure the temperature of the pressure inlet, a sheathed R-type thermocouple was employed.

A functional block diagram is illustrated in Fig. 14, whereas main specifications are listed in Table 2.

3. 4 Measurement accuracy

Measurement accuracy was estimated for the requirement concerning a measurement altitude range covering approximately 120~75km of the high-altitude pressure sensor. The results obtained from the above are listed in Table 3. The overall

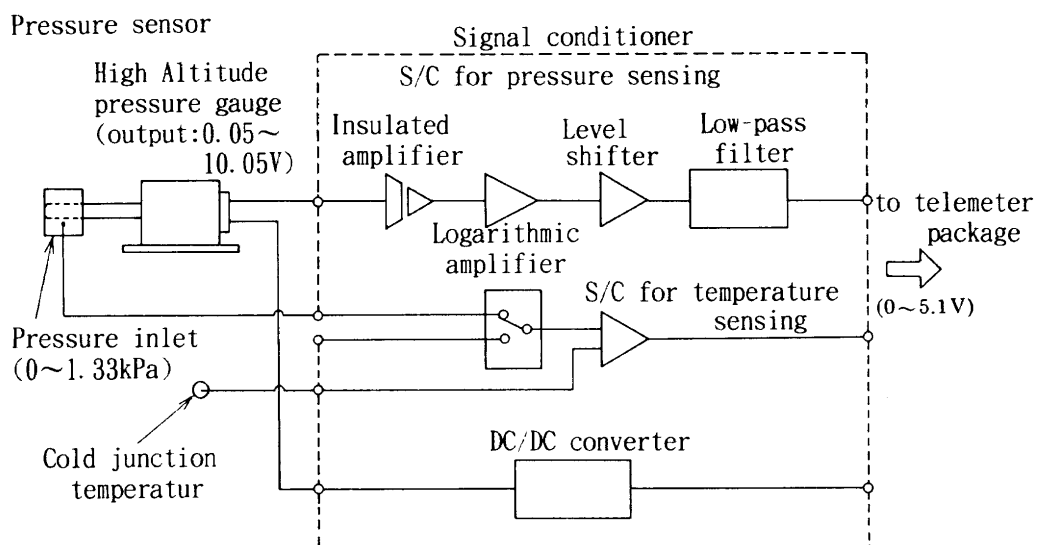


Fig. 14 Functional block diagram of signal conditioner

Table 2 Specifications of S/C

Input range	0.01~+10V
Excessive input	maximum 15V (at atmosphere)
Output level	0~5.1 ±0.1V F.S.
Filter characteristics	cut-off frequency 0.31Hz, 0~3db
Output impedance	less than 1kΩ
Power source voltage	18~34VDC
Consumed current	Maximum 110mA

Table 3 Measurement requirement and measurement accuracy of measurement system

	Measurement requirement		Measurement accuracy (%F.S.)			
	Measurement range	telemeter output accuracy	sensor	S/C	telemeter package	total
Pressure	0.533~1333Pa	±2.5%	±1.6%	±1.1	±1.2	±2.2
Temperature	0~750°C	±3.0%	±0.4%	±0.89	±1.2	±1.5

measurement accuracy of the pressure sensor equipped onto the vehicle is within ±2.5% stipulated in the measurement requirement sheet, and the measurement requirement is satisfied. For assessment of the overall accuracy (A_t), the equation shown below was used.

$$A_t = \sqrt{(A_s)^2 + (A_{s/c})^2 + (A_{tp})^2} \quad (2)$$

, where

A_s : sensor accuracy

$A_{s/c}$: S/C accuracy

A_{tp} : telemeter package accuracy

4. Ground tests

As environment condition during the flight of OREX launched by H-II rocket, that for condition of H-II rocket was applied both on a level of the acceptance test (AT) and on a level of the qualification test (QT). The pressure sensor and signal conditioner are exposed to all the environments not only in case of launching by H-II rocket but also in case of separation from the rocket, deorbiting, and re-entry into the atmosphere. To accomplish the design adequate enough to enable these devices to endure the environments, environment condition each sensor vehicle should be established and avoidance of trouble should be confirmed by tests (or by analysis depending on circumstances).

In environment tests of the pressure sensor, fundamental-performance-confirming tests and temperature test of the pressure sensor were repeated whenever each test of vibration, shock, heat, vacuum, etc. was made. Tests were further promoted with comparison of the test results with the initial fundamental data, checking to see if the functions of the pressure sensor was normal enough. In the vibration/shock tests, a test of the pressure sensing system in the triaxial direction was conducted. The triaxial direction, i.e. the direction of the X, Y, and Z axes in the environment test is given in Fig. 15. In the fundamental performance confirmation test, acquisition was made with drift characteristic data, compared data with the values shown in the calibrated standard pressure gauge, responsive characteristic data for the

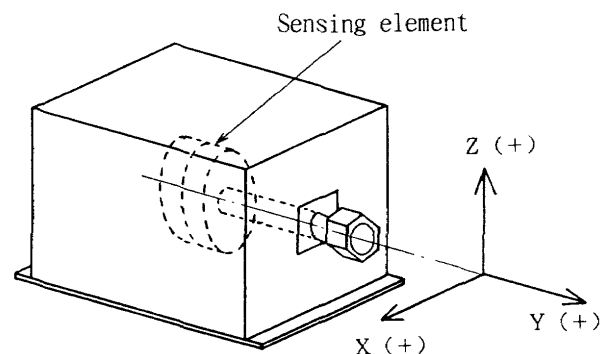


Fig. 15 Definition of triaxial direction in vibration/shock test

vibration or shock while the pressure gauge is in action, etc., and it is confirmed that functions are all in normality.

4.1 Environment test

In the technology test for environmental performance confirmation with a set of the pressure gauge, responses for temperature and random vibration were examined. In the temperature test, characteristics under atmospheric pressure at room temperature and temperature characteristics in both the inside and the outside of the pressure gauge in a vacuum chamber together with pressure gauge output temperature characteristics were examined. Tests of the pressure gauge temperature distribution characteristics/drift characteristics under the vacuum environment (0.00133Pa in the vacuum chamber) were conducted for approximately 65 minutes after the pressure sensor power was supplied. The result obtained in the above is shown in Fig. 16. The power I.C. whose temperature was elevated to the highest reached a stationary value of 60°C 40 min after the power was supplied. It is confirmed that drift of the pressure gauge output is stabilized 25 min after the power was supplied.

The pressure gauge temperature cycle test under vacuum environment (the pressure value in the vacuum chamber is 1.33Pa) was conducted at temperature cycle of 24°C, 54°C, -8°C, and 54°C in the vacuum chamber. The result of this test is shown in Fig. 17. Measurement was carried out

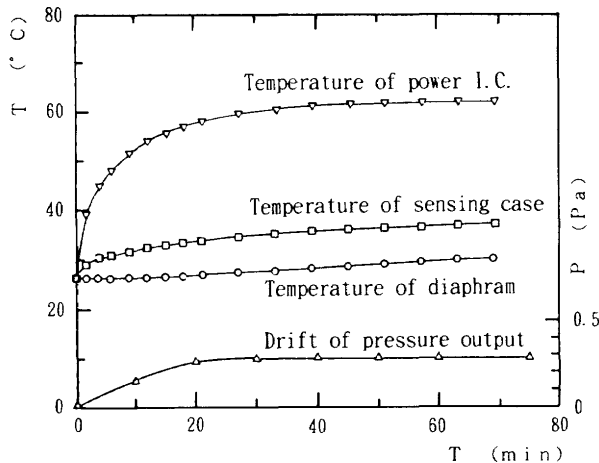


Fig. 16 Pressure sensor temperature distribution characteristics/drift characteristics

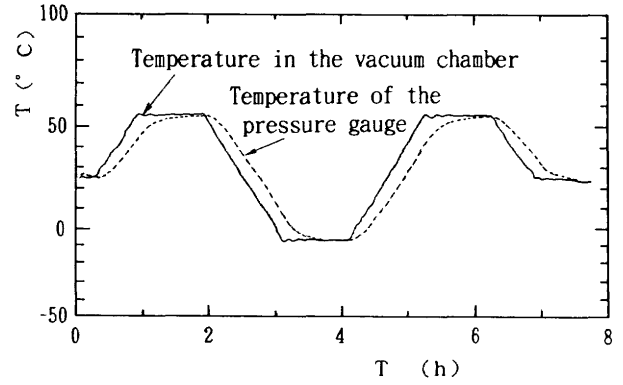


Fig. 17 Pressure gauge temperature cycle test

Table 4 Random vibration test condition

Test level	Condition
AT/100	20~180Hz:6db/oct 180~400Hz:0.085G ² /Hz 400~2000Hz:-6db/oct 3 axis, 30sec/axis
AT	20~180Hz:6db/oct 180~400Hz:0.85G ² /Hz 400~2000Hz:-6db/oct 3 axis, 60sec/axis
QT	20~180Hz:6db/oct 180~400Hz:3.4G ² /Hz 400~2000Hz:-6db/oct 3 axis, 120sec/axis

during the test with the temperature, power and output voltage of the pressure gauge to find that nothing abnormal occurred.

In the random vibration test, a triaxial/3-direction test was conducted at frequency 20~2kHz, test level AT/100, and AT and QT. The random vibration test condition is listed in Table 4. From the random vibration test, resonance frequencies were observed at approximately 500~2000Hz with respect to the individual axes. The result of the random vibration test in the pressure gauge X-axis "+" direction at the level AT/100 is shown in Fig. 18.

The temperature test and random vibration test as an acceptance level test was cleared. In addition to the above, an electromagnetic compatibility test was executed to examine the adaptability for electromagnetic interference. Thus it is confirmed that the functions before and after the test

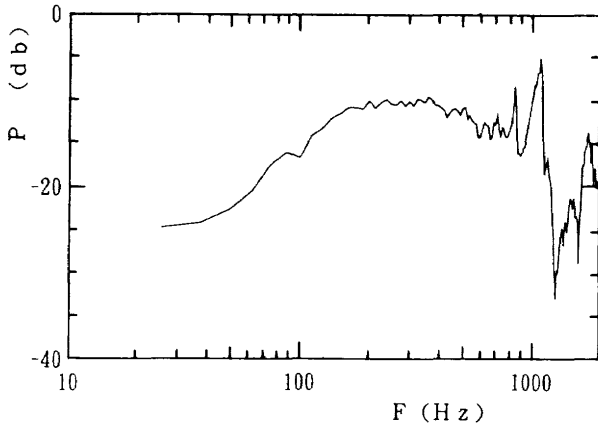


Fig. 18 Pressure gauge/random vibration test (X axis "+")

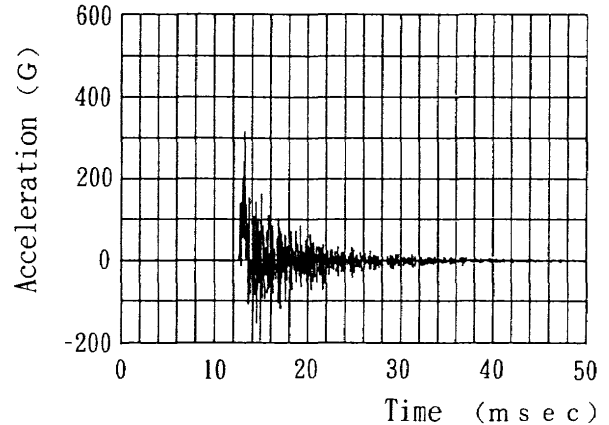


Fig. 19 Acceleration in an impact test (Y axis "+") with time

are normal.

In the technology test for environment performance confirmation of the pressure sensor to be equipped onto OREX, random frequency and Charpy impact response were examined. The test was conducted under the same condition as that of the pressure gauge single-set test in case of the random vibration test. In case of the Charpy impact test, a test was conducted in triaxial 6 directions at frequency 100~400Hz, the maximum acceleration 500G, test level AT/10, AT, and QT. The Charpy impact test condition is listed in Table 5. The results of the acceleration of the pressure sensor for Charpy impact test (Y axis "+") complying with time and the acceleration complying with the frequency are shown in Figs. 19 and 20, respectively. During this impact test, measurement of the consumed current of the pressure sensor and output voltage was carried out. The result of the above measurement is shown in Fig. 21.

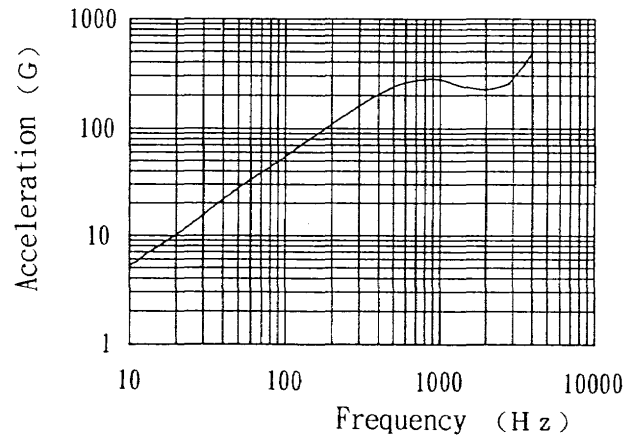


Fig. 20 Acceleration in an impact test (Y axis "+") with frequency

With the pressure sensor when impact is applied, none variation in the consumed current and output voltage was noticed. From this it is confirmed that everything is free from abnormality. From the random vibration test and Charpy impact test, the approved level was cleared. Thus it is understood

Table 5 Charpy impact test condition

Test level	Condition
AT/10	100~1500Hz: 6db/oct 1500~4000Hz: 50G 3 axis 6 directions, 1turn/axis, Q=10
AT	100~1500Hz: 6db/oct 1500~4000Hz: 500G 3 axis 6 directions, 1turn/axis, Q=10
QT	100~1500Hz: 6db/oct 1500~4000Hz: 500G 3 axis 6 directions, 1turn/axis, Q=10

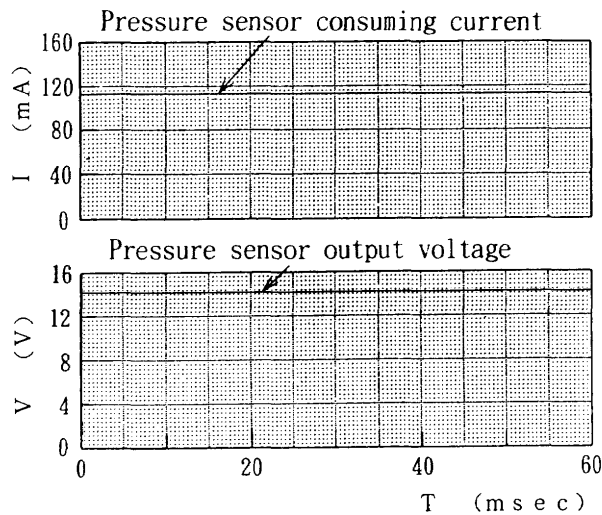


Fig. 21 Pressure sensor consuming current/
output voltage records at the impact test
(Y axis "+")

that the functions of the sensor is normal.

In addition to the above, a modal survey test for application of vibration was conducted, and resonance frequency data of the 3 axes of the pressure gauge and sensor diaphragm were obtained by filling up the pressure of approximately 65Pa into the pressure gauge. From the data, it is revealed that the individual resonance frequency is 500~1000Hz. As a result, it is confirmed that great deviation of those frequencies are made from the resonance frequency 45Hz of the OREX vehicle, and that everything is free from resonance problems. On the other hand, it is concluded from analysis that the strength margin value is sufficiently large positive for either of the elements. As a result, it is confirmed that pressure measurement during the flight of OREX is possible thanks to the environment test after remodeling. It is also confirmed that the pressure gauge is robust enough to endure the vibration, shock, etc. in launching H-II rocket.

4.2 Fundamental performance confirmation test

In the fundamental performance confirmation test, span confirmation and calibration were examined with respect to the pressure sensor to be equipped onto OREX by using rectified standard fundamental pressure gauges at National Research Laboratory of Metrology, Ministry of International

Trade and Industry (MITI). Concurrently with this, acquisition of the characteristic data was made with the sub-standard pressure sensor to be used for the function tests henceforth. Baraton Co.'s 398H type whose pressure range is 0~1.33kPa was used as the standard pressure gauge PS, and the pressure gauge P1~P3 to be calibrated are all Barocell type manufactured by Edwards Co.

4.2.1 Span confirmation test

Elevation and reduction of pressure ranging from the 0 point to the rated full scale of the individual pressure sensors were made to confirm the span and hysteresis of the individual sensors.

The span accuracy test results are listed in Table 6.

Table 6 Pressure gauge and span accuracy

Pressure gauge	Span accuracy
P1 : 590AB type 0~133Pa	$\pm 0.1\%$
P2 : 600 type 0~1.33kPa	-0.1%
P3 : 590 type 0~1.33kPa	$\pm 0.5\%$

P1 and P2 of the pressure gauge to be rectified are available as sub-standard, whereas P3 is a pressure gauge to be equipped onto OREX.

4.2.2 Pressure gauge rectification test

The pressure gauge rectification was made with the pressure sensor P1~P3 rectified in a pressure range from 0.13Pa (0.001Torr) to 1.33kPa (10Torr). Rectification results of the pressure sensor to be equipped onto OREX are shown in Fig. 22. With the pressure gauge P3 to be equipped onto OREX, the reading accuracy complying with the one of the standard pressure gauge was within approximately +0.5% in the individual pressure values.

From the above test results, confirmation was made as shown below.

1) A characteristic test result reveals that drift variation of the pressure gauge becomes stabilized approximately 30 min after power is supplied. Based on this fact, it is arranged that supply of power onto the pressure gauge will be made 2800 sec before starting measurement at an altitude

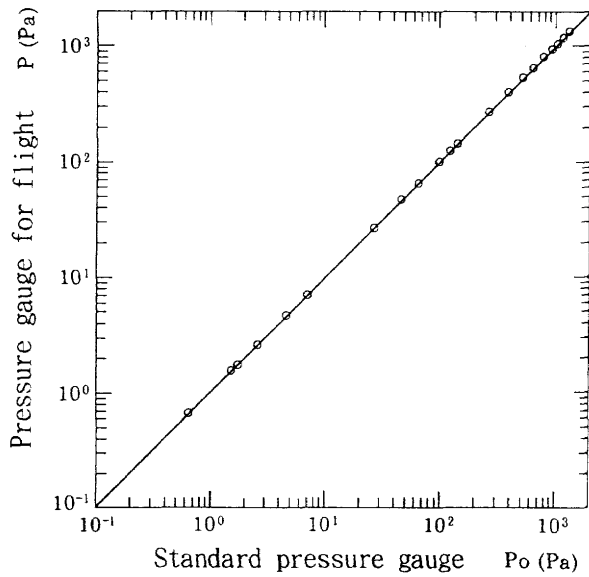


Fig. 22 Calibration result of pressure gauge for flight

120km.

2) Shock test or the vibration test result of the environment test reveals that a shift range of the off-set is in the maximum ± 50 mv. Owing to the above fact, measurement is possible within the characteristic range of the pressure sensor S/C. Furthermore to allow the measurement resolution to be heightened as far as possible, the variable resistor for adjustment of the off-set of the pressure gauge was set to the off-set value $E_{\text{off}} = 50$ mV at the pressure value nearly equal to 0.0 After that, the resistor was fixed by a bonding agent.

4. 2. 3 Tests after installation and launching site function confirmation

The function confirmation tests of the pressure sensor system was conducted after installation using a pressure confirmation test unit in Mitsubishi Heavy Industry's Nagoya Factory. In the meanwhile, the final test was conducted before launching of H-II rocket in the launching site in Tanegashima Space Center. The pressure confirmation unit is comprised of a vacuum pump, pressure gauges, pressure adjustment valves, flanges, etc. A schematic diagram of the arrangement of these devices is illustrated in Fig. 23. An absorption pump was employed in order to obtain clean and pure vacuum where none of oil vapor is allowed to be produced with an aim of preventing various

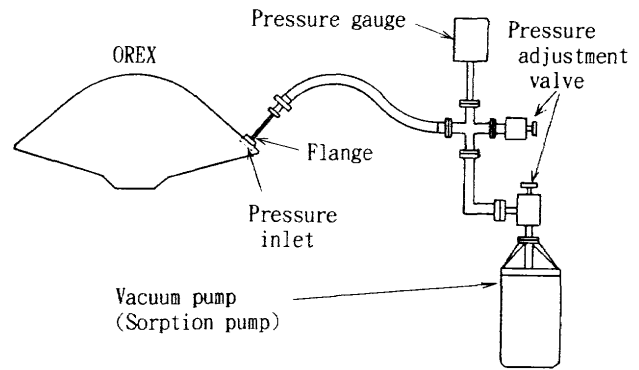


Fig. 23 Schematic diagram of pressure confirmation test unit

types of control equipment and apparatus, a variety of measurement instruments, etc. equipped onto OREX from being contaminated. The absorption pump, which is devoid of portions to be driven into mechanical motion and is free from oil, mercury, etc. in usage, can give vacuum as clean and pure as $0.1 \sim 0.01$ Pa starting from an atmospheric state under a vibration-free and noiseless condition. Adsorption of the gas in the inside of the pump is made by filling an adsorbing agent into the body of the pump on the exhaust unit and by making cooling with liquid nitrogen (-196°C) from the outside, by which exhausting is completed. The amount of the gas to be adsorbed by the absorption pump is a restricted one, and

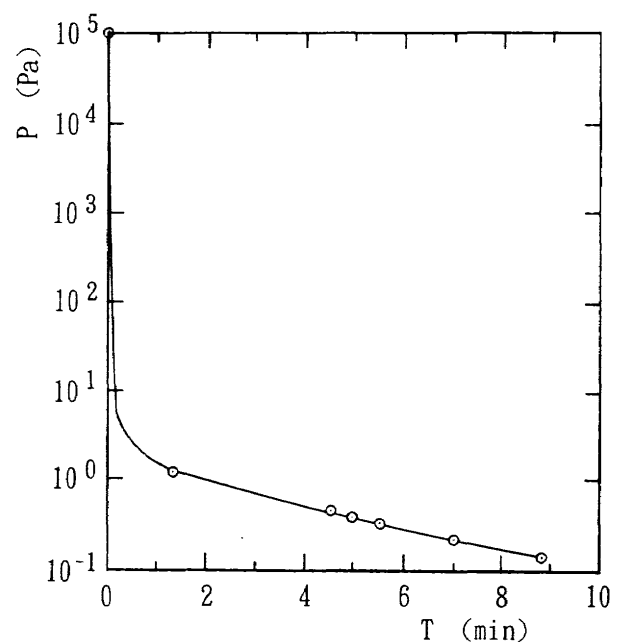


Fig. 24 Diagram of exhaust characteristics of pressure confirmation test unit

the maximum volume of the exhaust of the pump used is 40 ℓ. A schematic diagram of the exhaust characteristics in a state where the flanges of the pressure confirmation unit is made blind is shown in Fig. 24.

Confirmation was made with the functions of the pressure sensor system through with the output value of the telemeter corresponding to the applied pressure value by pressing the flanges of the pressure confirmation unit onto the pressure inlet surface of the pressure sensor via an O-ring and by applying the pressure in a pressure sensor action range. The result of the function confirmation test in the launching site is depicted by ○ marks in Fig. 25. At the pressure whose applied pressure value is higher than approximately 30Pa, the applied pressure and the telemeter output value coincide with each other. However in the region where the applied pressure value is lower than approximately 30Pa, the telemeter pressure value is higher than the applied pressure value. This is because of the fact that leakage is made between the flanges and the surface of the OREX pressure inlet, which is coated with zirconia so that the device can endure aerodynamic heating at the reentry into the atmosphere. Roughness of the zirconia surface, i.e. the pressure inlet surface coming into contact with the O-ring of the flange, induced the leakage.

From these test results, it was confirmed

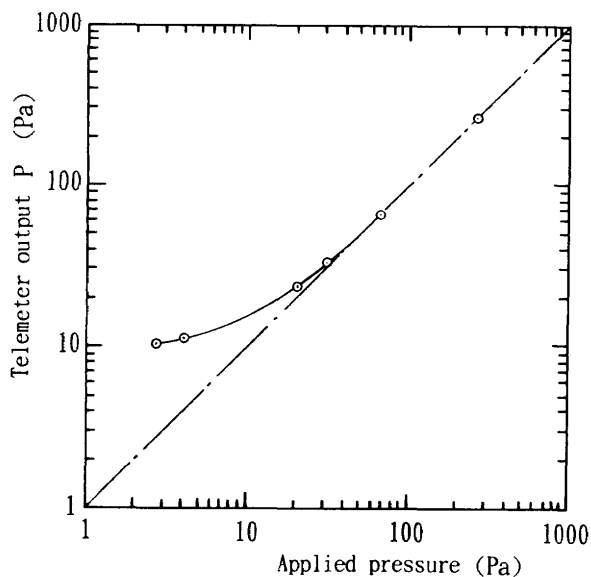


Fig. 25 Result of function confirmation test at the launching site

that the functions of the pressure system after the installation and in the launching site was normal enough.

5. Flight test results

OREX splashed down on the scheduled waters after completing the flight on the planned orbit after being separated from H-II rocket. It is found from the telemetered data of IMU that the angle of attack of the vehicle was $2^{\circ} \sim 3^{\circ}$ around 120km high, and hereafter remained less than 1° until 75km, the altitude limit of high-altitude pressure measurement. In this while, the planned experimental data were accepted with satisfaction, and the orbital re-entry experiment was finished. Reports concerning OREX's mission are available for reference in Literature 8. Supplying power to settle the drift of the pressure gauge amplifier from the gained flight data was made 46 min before reaching the altitude 120km where measurement was started, and thus the scheduled pressure measurement requirement condition was satisfied. The data acquisition of the off-set value of the pressure gauge electric system to be a criterion of the pressure measurement data was made in the vicinity of a point at the altitude of approximately 352km which can be regarded as vacuum after the lapse of more than 30 min after power was supplied. At the altitude around 350km, the pressure value is about 3 orders of magnitude lower than at the altitude less than 120km. Therefore if the off-set value (E_{off}) obtained at the altitude 352km is determined to be the pressure value $P=0$, then the data at the altitude less than 120km can be measured on the assumption that the error is less than 0.1%. The telemeter output value of the pressure gauge off-set value obtained at the altitude 400~352km was 68 counts. From the pressure gauge rectification result and characteristics of S/C, it is comprehended that a relational equation of S/C output S_{out} for the pressure value P is given as shown below.

$$S_{out} = 1.671 \times \log (P \times K + E_{off}) + 3.418 \quad (3)$$

where $K = 1/133.3$ (V/Pa). From the voltage conversion coefficient 0.02V/count and from Eq. (3), it is concluded that $E_{off} = 58.7\text{mV}$. The value is almost the same as the one obtained by being set

before launching OREX by H-II rocket. It follows from this that the minimum resolution of the pressure sensor system is 0.2185Pa. This allowed the 3.5 orders of magnitude measurement which had almost been expected to be performed. The high-altitude pressure data complying with the flight time of seconds that was telemeter-transmitted to the station on the Christmas Island are shown by count values in Fig. 26. It is confirmed that the said high-altitude pressure data are quite distinct ones even entirely free from electric noise. For the obtained data of the flight time of seconds, adjustment to allow the flight-mode-on time of seconds of an inertia measurement system (IMU), delay time by a low-pass filter of S/C, response delay by the pressure piping system, and the time difference in the frame of the telemeter package are required. These adjusted values are listed in Table 7. When a signal causing more rapid time change is inputted with the low-pass filter, deformation of the waveform is generally accompanied. However it is elucidated that inverse-filter analysis allows the said deformation to be represented as group delay characteristics⁹⁾. As a result, signal reproduction was made with great ease and with high ac-

curacy.

With the data of the time of seconds, reproduction was individually made from the flight data. In the meanwhile with the high-altitude pressure data, calculation of the pressure values was made from the telemeter output in accordance with Eq. (3). A result of the temperature record on the pressure inlet for the obtained altitude is shown in Fig. 27. With the temperature data of the thermocouple attached onto the pressure inlet, it is noticed that the temperature remains 18° constant at the altitude ranging from 120km to 82km. At the altitude 82km, the temperature was started to be gradually elevated and reached 25°C at the altitude 75km. From this result, it is considered that no influence by the temperature in a rarefied gas region will be exercised on the transducer. These data were fed into the rarefied gas calculation.

Results of the ground speed¹⁰⁾ with the altitude that are obtained by NASDA are shown in Fig. 28. In the meantime, the high-altitude data¹⁰⁾ expressed at the time frame of seconds after-

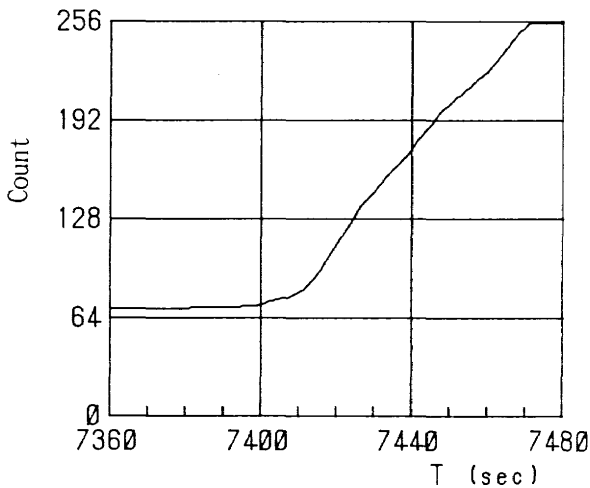


Fig. 26 Telemeter output of high-altitude pressure for flight time of seconds

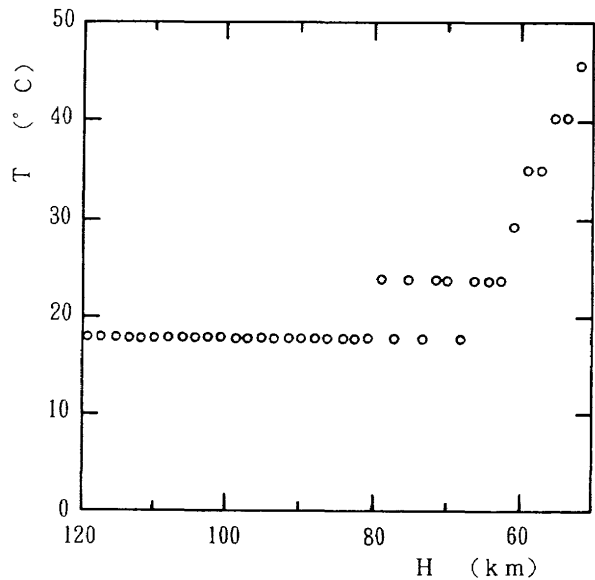


Fig. 27 Temperature of pressure inlet with altitude

Table 7 Rectification of time data

1) Rectification between time after IMU flight mode-on and lift-off	-39.725 sec
2) Delay time of S/C by low-pass filter	-2.2 sec
3) Response delay by pressure piping system (altitude 120~75km)	-0.34~-0.014 sec
4) Access time difference of telemeter package in a frame	0.508 sec

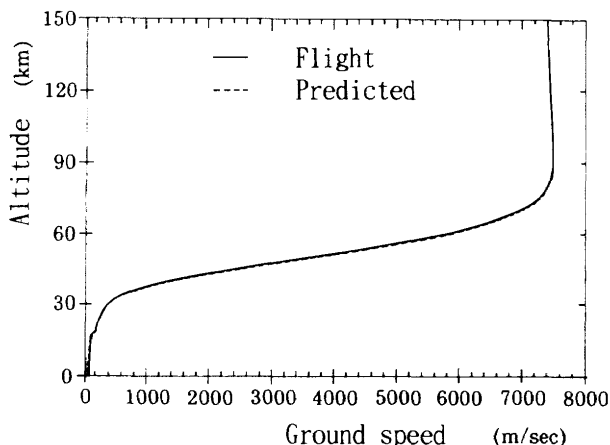


Fig. 28 Ground speed versus altitude

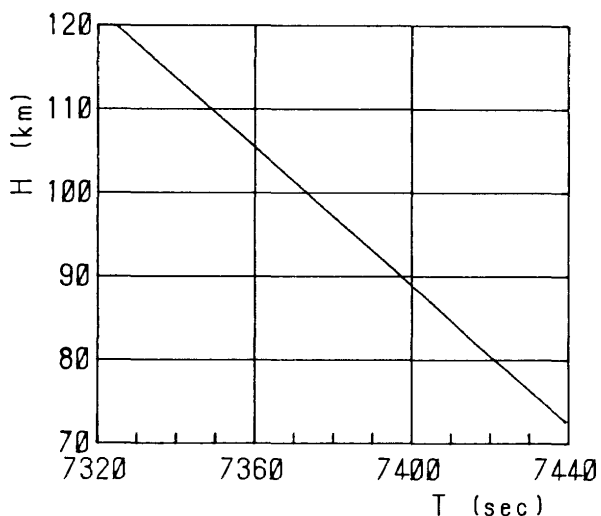


Fig. 29 Time of seconds after launching and altitude

launching are shown in Fig. 29. From the altitude data for the after-launching time of seconds and the measured data of the high-altitude pressure for the data of the time of seconds, a relation between the altitude pressure data and the high-altitude data was obtained. This is shown in Fig. 30. The solid line indicates the result of the flight-pressure history. At the altitude 100km, the pressure values of the flight data are shown in a style of a belt. This denotes the resolution of the pressure measurement. In this connection, the data obtained at the altitude 120~115km give 2 counts. From the measurement resolution, it is perceived that the pressure values in question are between 0.33Pa and 0.5578Pa. The values shown by a broken line for the sake of comparison with the flight data are derived from CFD analytical results by the Navier-Stokes (N-S) code¹¹⁾, and by

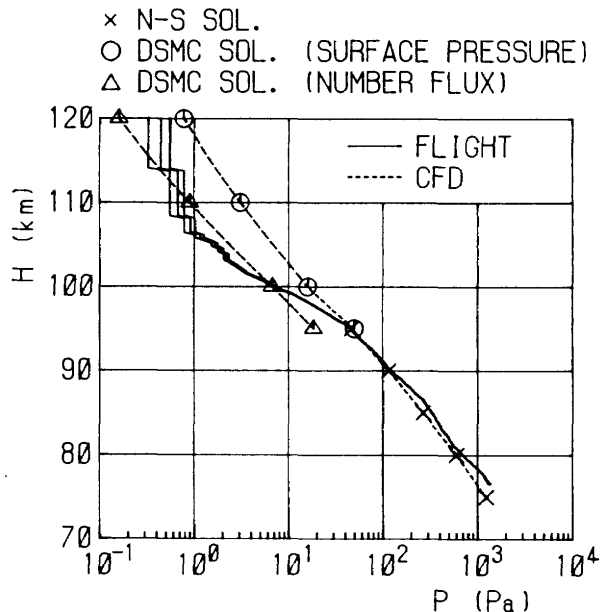


Fig. 30 High-altitude pressure for altitude

the direct simulation Monte Carlo (DSMC) code¹²⁾. Prediction (the x marks in Fig. 30) of N-S is almost close to the measurement at the altitude less than 95km, but the analytical results provide slight difference in the tendency of the change with the altitude. It is shown that the result of the DSMC wall surface pressure (the o marks in Fig. 30) at the altitude more than 95km is deviated from the measured data. DSMC analytical values are the predicted values of the wall surface pressure, not in the tube. At the altitude more than approximately 96km where rarefied-gas effect is remarkable, the wall surface pressure is different from the pressure obtained on an ending terminal of the inlet cold wall, i.e. the output value of this measurement. Composition of the pressure inlet system and both the pipe wall temperature and the gas temperature become effective. The fact referred to above is well known in the rarefied-gas field. The pressure in the pressure sensor inlet calculated from DSMC molecule flowing flux¹³⁾ is shown in Δ marks in Fig. 30. The pressure in question coincides with the flight data at the altitude 100~110km. However at the altitude 95km, deviation is noted because rarefied-gas effect cannot be applied.

NASDA performed wall surface pressure measurement in the middle-altitude region (the altitude approximately 80~50km) where aerody-

dynamic heating is very severe. A middle-altitude pressure sensor was equipped onto the 1st row of the ceramic tile. The place where the sensor was equipped is shown in Fig. 2. The middle-altitude pressure sensor is of the capacitance-diaphragm type, and its measurement pressure range is 0~30.39 kPa. In the meantime, the measurement accuracy of the device is 1.114kPa. The wall-surface middle-altitude pressure measurement data¹⁰⁾ with the altitude obtained by NASDA are shown in a dotted line in Fig. 31. The solid line indicates the high-altitude pressure. In Fig. 32, OREX wall-

surface pressure distribution obtained by Newtonian Flow Theory is shown in a single-point chain line. NAL's hypersonic wind tunnel data^{10) 14)} are shown in \circ marks in the same figure. Also shown by a broken line is a real-gas CFD prediction at 90km altitude. The flight data from high altitude pressure sensor at the same altitude is indicated by a solid mark normalized by CFD pressure value at stagnation point. Very good agreement between the measured and the predicted value is noted. The wall-surface pressure distribution non-dimensionalized by stagnation-point pressure is likewise shown in the figure. Although the experimental values are higher than the ones of Newtonian Flow Theory with the wall-surface pressure in the skirt part, almost the same values are shown with the wall-surface pressure on the positions of the high-altitude pressure hole ($\theta \approx 73^\circ$) and the middle-altitude pressure hole ($\theta \approx 55^\circ$). Also with the high-altitude pressure sensor and middle-altitude pressure sensor obtained from the flight data, the wall-surface pressure measurement values in the vicinity of the altitude 80km coincide with each other. From these facts, the results of the high-altitude pressure measurement performed as NAL mission and the middle-altitude pressure measurement carried out as NASDA mission are believed to be excellent ones.

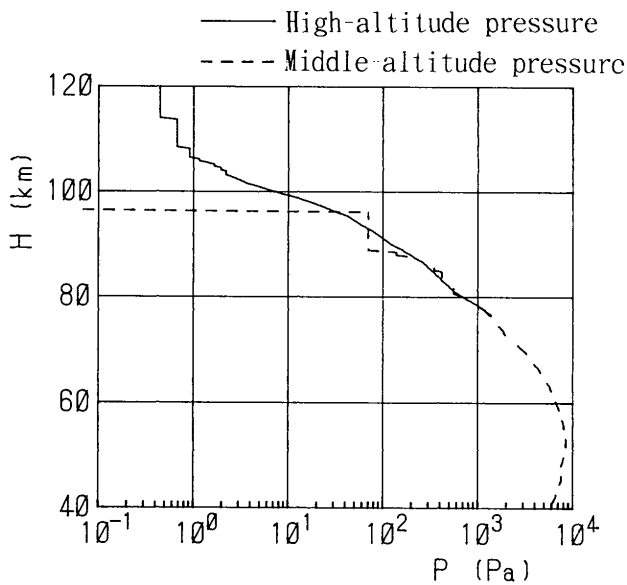


Fig. 31 Middle-altitude pressure/high-altitude pressure for altitude

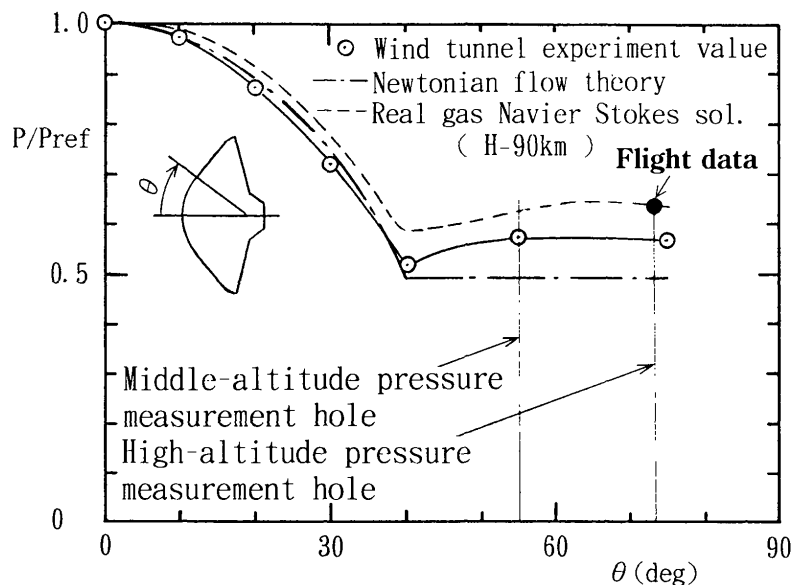


Fig. 32 OREX wall surface pressure distribution

6. Conclusions

The first re-entry experiment in our country was conducted with OREX, and the scheduled high-altitude wall surface pressure data were obtained with considerable satisfaction. The high-altitude pressure data obtained were almost in agreement with the results of both N-S and DSMC, and the relation with the middle-altitude pressure sensor data obtained by NASDA was also excellent.

For a new space transportation system believed to be the one of infrastructures of Japan's space development in future, winged space planes that are usable repeatedly are in consideration. Researches and development plans for such places have already been started. For the optimum design to accomplish the operations of the space vehicles under the flight environment full of variety and severity ranging from being launched into space to landing an airfield, acquisition of the re-entry environment data and establishment of prediction methods with reliability in aerothermodynamic characteristics are indispensable. Pressure is one of the most fundamental quantities in such data and methods, and the high-altitude pressure measurement conducted as a measurement mission of OREX realizing the acquisition of the high-altitude pressure data as the fundamentals of the aerodynamic environment was very much of significance. The technology and knowledge concerning the measurement of the pressure in a region of rarefied real gas at the re-entry are the ones with which application to other fields of technology can be expected.

7. Acknowledgments

The authors of this paper are very grateful to Mr. Toshio Akimoto, Associate Senior Engineer of NASDA who has been kind enough to provide the authors with a variety of precious instruction in promoting the OREX plan. The authors are also thankful to Messrs. Hidemi Yasui, Masashi Kunimi, and Hiroki Hara, Engineers of Nissan Motor Co., Ltd. who have been cooperative to the authors in designing the system of the measurement mission series and in conducting ground based environment tests. The authors' appreciation is extended

to Mr. Akira Oiwa of National Research Laboratory of Metrology, Agency of Industrial Science and Technology, MITI who has kindly furnished the authors with constructive advice and useful suggestions by operating rectifying units in which standard equipment and apparatus are contained for high-accuracy rectification of the pressure gauges.

References

- 1) Siemers, P.M. et al.; Shuttle Flight Pressure Instrumentation: Experience and Lessons for the Future, in NASA Conference Publication 2283 "SHUTTLE PERFORMANCE: LESSONS LEARNED," March 1983
- 2) Throckmorton, D.A.; Shuttle Entry Aerothermodynamic Flight Research: The Orbiter Experiments Program, Journal of Spacecraft and Rockets, Vol. 30, No. 4, pp. 449-465, 1993
- 3) Koppenwallner, G.; BREM-SAT: A small reentry satellite for rarefied gas dynamic research, Proceedings of ISRGD, 1990
- 4) Orbital Re-entry Experiment Sub-group of NAL/NASDA Joint HOPE R & D Team; A Report concerning Completion of Orbital Re-entry Experiment Project Development, 1993 (in Japanese)
- 5) Onji, X., Yamamoto, M., and Tsuda, H.; Analytical and Experimental Studies of Free Molecule Impact Pressure Probe, NAL Report TR-474, 1976 (in Japanese)
- 6) Patterson, G.M.; Theory of free-molecule, orifice type, pressure probes in isentropic and nonisentropic flows, UTIA Report No. 41, 1956, University of Toronto
- 7) Soga, K. and Onodera, N.; Influence of Pressure Holes Exercised on Time Delay of Pressure Measurement, Papers of NAL TM-238, 1972 (in Japanese)
- 8) Inouye, Y., Watanabe, Y., Wada, Y., Akimoto, T., and Yasui, H.; Some Aerothermodynamic Measurement Results of the Orbital Re-entry Experiment (OREX), ISTS 94-d-24, proc. of 19th ISTS, pp. 431-439, 1994
- 9) Oppenheim, A. V. & Schafer, R. W.; Digital Signal Processing (Book 1), Corona Publishing Co., pp.

- 41~, 1978 (translated to Japanese)
- 10) NAL/NASDA HOPE Joint Research Team; Papers of HOPE/OREX Workshop Lectures, NAL SP-24, 1994 (partly in English)
 - 11) Wada, Y.; Actual Gas Analysis...6.2.3. Calculation around OREX from Report concerning Achievements of NAL/NASDA Joint Researches, Study on HOPE- (No. 10) Study on Aerodynamic Characteristics (01 HOPE Aerodynamic Numerical Analysis), NAL/NASDA, 1991 (in Japanese)
 - 12) Koura, K.; Rarefied Gas Flow Simulation around OREX and HOPE by Rarefied Gas Numerical Air Tunnels, Report concerning Achievements of NAL/NASDA Joint Researches ... (No. 10) Study on Aerodynamic Characteristics (01 HOPE Aerodynamic Numerical Analysis), NAL/NASDA, 1991 (in Japanese)
 - 13) Koura, K.; Rarefied Atmosphere Flight Data and DSMC Analysis, Report concerning Achievements of NAL/NASDA Joint Researches, Study on HOPE (No. 15), Orbital Re-entry Experiment (OREX), NAL/NASDA, 1995 (in Japanese)
 - 14) Shimoda, T.; Wind Tunnel Tests, Report concerning Achievements of NAL/NASDA Joint Researches, Study on HOPE, (No. 15), Orbital Re-entry Experiment (OREX), NAL/NASDA, 1995 (in Japanese)

TECHNICAL REPORT OF NATIONAL
AEROSPACE LABORATORY
TR-1287T

航空宇宙技術研究所報告1287T号 (欧文)

平成8年4月発行

発行所 航空宇宙技術研究所
東京都調布市深大寺東町7-44-1
電話 三鷹(0422)47-5911(大代表) 〒182
印刷所 株式会社 共 進
東京都杉並区久我山5-6-17

Published by
NATIONAL AEROSPACE LABORATORY
7-44-1 Jindaiji higashi, Chōfu, Tokyo 182
JAPAN

Printed in Japan